

Data-driven Modeling and Inference for Bayesian Gaussian Process ODEs via Double Normalizing Flows

Jian Xu, Delu Zeng

Abstract

Recently, Gaussian processes have been used to model the vector field of continuous dynamical systems, referred to as GPODEs, which are characterized by a probabilistic ODE equation. Bayesian inference for these models has been extensively studied and applied in tasks such as time series prediction. However, the use of standard GPs with basic kernels like squared exponential kernels has been common in GPODE research, limiting the model’s ability to represent complex scenarios. To address this limitation, we introduce normalizing flows to reparameterize the ODE vector field, resulting in a data-driven prior distribution, thereby increasing flexibility and expressive power. We develop a data-driven variational learning algorithm that utilizes analytically tractable probability density functions of normalizing flows, enabling simultaneous learning and inference of unknown continuous dynamics. Additionally, we also apply normalizing flows to the posterior inference of GP ODEs to resolve the issue of strong mean-field assumptions in posterior inference. By applying normalizing flows in both these ways, our model improves accuracy and uncertainty estimates for Bayesian Gaussian Process ODEs. We validate the effectiveness of our approach on simulated dynamical systems and real-world human motion data, including time series prediction and missing data recovery tasks. Experimental results show that our proposed method effectively captures model uncertainty while improving accuracy.

1 Introduction

Recent research has utilized machine learning algorithms to model the behavior of dynamical systems governed by continuous-time differential equations [Hegde *et al.*, 2022; Chen *et al.*, 2018; Zhu *et al.*, 2022; Chen *et al.*, 2022; Zhang *et al.*, 2022; Heinonen *et al.*, 2018]. Mathematically, it can be written as,

$$\frac{d\mathbf{x}(t)}{dt} = \mathbf{f}(\mathbf{x}(t)) \quad (1)$$

where $\mathbf{x}(t) \in \mathbb{R}^d$ represents the latent state, and \mathbf{f} represents the vector field. One of the most promising approaches is the use of Gaussian process (GP) vector fields to learn unknown nonlinear differential functions from state observations in a Bayesian manner, referred to as GPODEs [Hegde *et al.*, 2022; Heinonen *et al.*, 2018]. In these dynamical system models, the vector fields are endowed with Gaussian process priors, allowing for the learning of unknown parameters.

Accuracy and uncertainty are crucial metrics in time series and dynamical system tasks to ensure the reliability and effectiveness of models. The limitations of previous GPODEs methods mainly lie in two aspects. Firstly, the learning of previous GPODEs was constrained by the modeling capacity. By assuming the vector field \mathbf{f} as a standard Gaussian Process with elementary kernels as prior, this limitation restricts the flexibility in modeling complex systems. Secondly, the inference of previous GPODEs endowed the augmented variational parameters with mean-field Gaussian posteriors. However, according to Bayes’ theorem, the posterior is often non-Gaussian, which may lead to errors in uncertainty estimation during inference.

To address these limitations, we incorporate normalizing flows to reparameterize the vector field of ODEs, resulting in a more flexible and data-driven prior distribution. Normalizing flow [Kobyzev *et al.*, 2020; Papamakarios *et al.*, 2021; Zhang and Chen, 2021; Maroñas *et al.*, 2021] was originally proposed to transform a simple random variable into a more complex one by applying a sequence of invertible and differentiable transformations. For the complex system dynamics that a standard GP equipped with elementary kernels cannot model, a good way is to transform the GP prior. Specifically, by applying the same idea as the normalizing flow on random variables, we transform the standard GP, \mathbf{f} , to get a more flexible and expressive random process. Additionally, due to the powerful flexibility of normalizing flows, we apply them to the posterior inference of GP ODEs, generating a non-Gaussian posterior. Through these dual applications of normalizing flows, our model improves accuracy and uncertainty estimates for Bayesian Gaussian Process ODEs.

Specially, we leverage the benefits of the analytically tractable probability density functions of normalizing flows to construct an interpretable and tractable variational learning algorithm that allows for simultaneous, precise, and reliable learning and inference of the unknown continuous dy-

namics. The effectiveness of our approach is demonstrated on simulated dynamical systems and real-world human motion data, including tasks such as time series prediction and missing data recovery. The experimental results indicate the superiority of our proposed method over previous methods in terms of accuracy and uncertainty estimation.

Overall, our contributions are as follows,

- We introduce double normalizing flows, a new perspective on the use of normalizing flows in Bayesian modeling of dynamical systems, presenting a flexible and data-driven framework for modeling complex systems.
- We develop a data-driven variational learning algorithm that utilizes the analytically tractable probability density functions of normalizing flows to enable simultaneous learning and inference of unknown continuous dynamics.
- We demonstrate the effectiveness of the proposed method on simulated dynamical systems and real-world human motion data, improving prediction accuracy and uncertainty estimation.

2 Related Works

The subsequent sections provide an overview of the existing literature on ODEs and normalizing flows, as well as their relationships.

Non-parametric ODE models Research has explored combining GP priors [Heinonen *et al.*, 2018; Hegde *et al.*, 2022] with ODEs for model specification. These approaches offer flexible and non-parametric ways to model complex dynamics in various applications. Specifically, [Heinonen *et al.*, 2018] proposes learning unknown, non-linear differential functions from state observations using Gaussian process vector fields, with the assumption that the vector field is a random function drawn from a Gaussian process. They provide a method to parameterize the ODE model with inducing points and use adjoint sensitivity equations to efficiently compute gradients of the system. Building on this, [Hegde *et al.*, 2022] proposes a Bayesian perspective for posterior inference of the model and a probabilistic shooting augmentation to enable efficient inference for long trajectories.

The relationship between normalizing flows and dynamic modeling Normalizing flows, as a class of generative models, have been shown to be flexible and expressive, allowing for complex and high-dimensional data modeling. Several studies have proposed using normalizing flows to enhance dynamic modeling. For example, [Deng *et al.*, 2020; Deng *et al.*, 2021] proposed a type of normalizing flow driven by a differential deformation of the Wiener process, which inherits many appealing properties of its base process. [Zhi *et al.*, 2022] proposed learning an ODE of interest from data by viewing its dynamics as a vector field related to another base vector field by an invertible neural network, from a perspective of differential geometry.

The relationship between normalizing flows and GP models [Maroñas *et al.*, 2021] introduced the Transformed Gaussian Processes (TGP) framework, which combines

Gaussian Processes (GPs) as flexible and non-parametric function priors with a parametric invertible transformation. The primary objective is to expand the range of priors and incorporate interpretable prior knowledge, including constraints on boundedness. In a subsequent work, [?] applied the TGP framework to create non-stationary stochastic processes that are inherently dependent. The TGP approach demonstrates particular suitability for addressing multi-class problems involving a substantial number of classes. While our paper also incorporates the idea of TGP, our approach differs in the sense that our baseline is a continuous dynamical system. Moreover, we consider the complexity of the posterior distribution and propose a novel approach called double normalizing flows, which further improves the model’s uncertainty estimation in time series prediction.

3 Method

In this section, we propose a Bayesian model to infer posteriors and other parameters on implementing vector fields using our double normalizing flows.

3.1 Gaussian Process ODEs

Gaussian Process ODEs are a class of nonparametric models used for modeling continuous dynamic systems that evolve based on vector fields with uncertainties. The fundamental concept of GP ODEs is to represent the unknown vector field as a Gaussian process prior, characterized by a mean function and a covariance function that governs the smoothness, volatility, and randomness of the stochastic function at different input points. Then, a numerical ODE solver can be used to compute the evolution of the stochastic function as samples over time.

The formulation of a GP ODE model involves specifying a prior distribution over the latent function \mathbf{f} and a likelihood function that establishes the relationship between the observed data and the latent function. More precisely, the model is defined by a zero-mean multidimensional Gaussian process prior over \mathbf{f} :

$$\frac{d\mathbf{x}(t)}{dt} = \mathbf{f}(\mathbf{x}(t)) \quad (\text{differential equation}) \quad (2)$$

$$\mathbf{f}(\mathbf{x}(t)) \sim \mathcal{GP}(\mathbf{0}, K(\mathbf{x}(t), \mathbf{x}'(t))) \quad (\text{the prior}) \quad (3)$$

$$\mathbf{y}(t) \sim \mathcal{N}(\mathbf{x}(t), R) \quad (\text{likelihood function}) \quad (4)$$

In a GP ODE model, $\mathbf{x}(t) \in \mathbb{R}^d$ represents the latent state, i.e. the true observed data, while $\mathbf{y}(t) \in \mathbb{R}^d$ denotes the observations contaminated by an unknown noise, $K(\mathbf{x}(t), \mathbf{x}'(t)) \in \mathbb{R}^{d \times d}$ is a stationary covariance matrix function, $R \in \mathbb{R}^{d \times d}$ represents the observation noise, and $\mathbf{f}(\mathbf{x}(t)) \in \mathbb{R}^d$ represents the velocity field that characterizes the dynamics of the function over time.

Inference in GP ODE models entails computing the posterior distribution over the latent function \mathbf{f} given the observed data $\mathbf{y}(t)$. This can be accomplished through numerical integration and variational inference. For instance, a popular approach [Hegde *et al.*, 2018] involves employing the Runge-Kutta method for numerical ODE solving to obtain an estimate of the latent function, followed by variational inference to compute the posterior distribution.

3.2 The Potential Limitations of Gaussian Process ODE models

GP ODE models are powerful tools for modeling dynamic systems, especially in scenarios with irregularly sampled data and the need for uncertainty estimation.

However, a limitation of these models is the sensitivity of their performance to the choice of kernel functions, which should be carefully selected based on the specific problem at hand. When dealing with complex data structures, relying solely on elementary GP kernels as Gaussian priors may result in local underfitting, as these kernels may lack the flexibility to capture fine details and meet the requirements of modeling complex dynamical systems [Hu *et al.*, 2021]. Moreover, the general principles of machine learning [Bishop and Nasrabadi, 2006] and Bayesian inference [Fortuin, 2022] suggest that using overly simplistic priors can introduce bias in parameter estimation, leading to deviations from the true posterior distribution and potential underfitting issues. Furthermore, we have found that another limitation of the previous GP ODE models is that the complexity of the data and the non-Gaussian distribution of the posterior often pose difficulties in handling parameter inference. This is particularly challenging when using variational inference techniques, as it can be difficult to find a suitable posterior distribution family to describe such cases.

To address this challenge, we propose incorporating normalizing flows as a means to significantly enhance the flexibility and reliability of Gaussian Process ODE models. Normalizing flows transform a simple random variable into a more complex one by applying a sequence of invertible and differentiable transformations. For the complex system dynamics that a standard GP equipped with elementary kernels cannot model, a good way is to transform the GP prior. Specifically, by applying the same idea as the normalizing flow on random variables, we transform the standard GP, \mathbf{f} , to get a more flexible and expressive random process. Additionally, due to the powerful flexibility of normalizing flows, we apply them to the posterior inference of GP ODEs, generating a non-Gaussian posterior. Through these dual applications of normalizing flows, our model improves accuracy and uncertainty estimates for Bayesian Gaussian Process ODEs. In the next subsection, we will present our approach for enhancing the expressiveness of Gaussian Process ODE models using double normalizing flows, resulting in a more flexible and reliable modeling framework.

3.3 Double Normalizing Flows

Modeling : Normalizing Flows for a Priori Transformation

To address the limitations of the Gaussian Process ODEs model’s a priori expressiveness, we first transform the Gaussian process prior through a normalizing flow. Normalizing flows [Rezende and Mohamed, 2015] are a family of flexible and invertible transformations that can map a simple prior distribution to a more complex distribution. Specifically, let \mathbf{x} be a d dimensional continuous random vector, and $p(\mathbf{x})$ be the corresponding probability density distribution. Normalizing flow can help construct a desired, often more complex

and possibly multi-modal distribution by pushing \mathbf{x} through a series of transformations, i.e. $G_K(\mathbf{x}) = \mathbf{g}_K \circ \dots \circ \mathbf{g}_2 \circ \mathbf{g}_1(\mathbf{x})$.

By repeatedly applying the rule for change of variables, the initial density ‘flows’ through the sequence of invertible mappings. At the end of this sequence we obtain a valid probability distribution.

$$\ln p(G_K(\mathbf{x})) = \ln p(\mathbf{x}) - \sum_{k=1}^K \ln \left| \det \frac{\partial \mathbf{g}_k}{\partial G_{k-1}(\mathbf{x})} \right| \quad (5)$$

For example, due to its simple network structure, \mathbf{g}_k can be designed to be referred to as a Planar Flow [Papamakarios *et al.*, 2021], as shown in the following formula:

$$\mathbf{g}(\mathbf{x}) = \mathbf{x} + \mathbf{u}h(\mathbf{w}^\top \mathbf{x} + b), \quad (6)$$

where $\mathbf{u} \in \mathbb{R}^d$, $\mathbf{w} \in \mathbb{R}^d$, $b \in \mathbb{R}$ are free network parameters, $h(\cdot)$ is a non-linear smooth function. This transformation is invertible, and its Jacobian determinant can be computed efficiently,

$$\det \left| \frac{\partial \mathbf{g}}{\partial \mathbf{x}} \right| = \left| \det (\mathbf{I} + \mathbf{u}\psi(\mathbf{x})^\top) \right| = \left| 1 + \mathbf{u}^\top \psi(\mathbf{x}) \right| \quad (7)$$

Applying the same idea as the normalizing flow on random variables, we can also transform the standard GP $\mathbf{f}(\cdot)$ into a more flexible and expressive random process $G_K(\mathbf{f})(\cdot)$. Specifically, we form the vector field by first passing the state variable $\mathbf{x}(t)$ through a multidimensional Gaussian process:

$$\mathbf{f}(\mathbf{x}(t)) \sim \mathcal{GP}(\mathbf{0}, K(\mathbf{x}(t), \mathbf{x}(t)')) \quad (8)$$

We then apply the series of transformations G_K to the output of the Gaussian process:

$$\mathbf{f}(\mathbf{x}(t)) \rightarrow G_K(\mathbf{f}(\mathbf{x}(t))) = G_K \circ \mathbf{f}(\mathbf{x}(t)) \quad (9)$$

The resulting function $G_K \circ \mathbf{f}$ can be used as the vector field in the ODE model since it is a valid multivariate stochastic process in the same input space by Kolmogorov’s consistency theorem [Oksendal, 2013]. By compounding K such transformations, we obtain a transformed a priori that is a highly flexible and expressive representation of the original vector field.

To train the compound transformation, we propose to use variational inference [Blei *et al.*, 2017; Zhang *et al.*, 2018], which has several benefits over maximum likelihood estimation. In a traditional GP model, the log marginal likelihood is optimized in closed form. However, in the present framework, this quantity is intractable, and hence we resort to variational inference via the Evidence Lower Bound (ELBO). By maximizing the ELBO, we can approximate the true posterior distribution over the latent variables. This allows us to learn the parameters of the compound transformation in a tractable and scalable manner. Next, we will introduce how to construct an expressive approximation in the proposed model.

Inference: Normalizing Flows for a Posteriori Transformation

To infer the posterior distribution of the model, we propose a variational inference method based on the normalizing flows prior. Specifically, we use a hierarchical Bayesian framework

to model the observed data $Y = \{\mathbf{y}(t_1), \mathbf{y}(t_2), \dots, \mathbf{y}(t_N)\}$ as a noisy realization of the underlying hidden state $X = \{\mathbf{x}(t_1), \mathbf{x}(t_2), \dots, \mathbf{x}(t_N)\}$:

$$\mathbf{y}(t) = \mathbf{x}(0) + \int_0^t G_K \circ \mathbf{f}(\mathbf{x}(\tau)) d\tau + \epsilon \quad (10)$$

where $t_n \in [0, T]$, $G_K \circ \mathbf{f}$ is the vector field defined by the transformed Gaussian process prior, and $\epsilon \sim \mathcal{N}(0, R)$ is a Gaussian noise term. We assume a standard Gaussian prior distribution over the initial variable $\mathbf{x}(0)$, i.e. $p(\mathbf{x}(0)) = \mathcal{N}(\mathbf{0}, I)$.

To infer the posterior distribution of $p(\mathbf{f}(t)|Y)$ given the observed data Y , we adopt a variational inference approach. We aim to find a distribution $q(\mathbf{f}(t))$ that approximates the true posterior distribution $p(\mathbf{f}(t)|Y)$ by minimizing the Kullback-Leibler (KL) divergence between $q(\mathbf{f}(t))$ and $p(\mathbf{f}(t)|Y)$. Specifically, we use the variational sparse Gaussian process (SVGP) [Titsias, 2009; Hensman *et al.*, 2015; Mao and Sun, 2020; Liu *et al.*, 2020] method to speed up the computation and relax the dependence on data.

SVGP is a popular and effective approach for scalable Gaussian process inference, which introduces a set of inducing points $Z = \{z_1, z_2, \dots, z_M\}$ and inducing variables $U = \{u_1, u_2, \dots, u_M\}$ with a prior distribution $p(U) = \mathcal{N}(0, K(Z, Z'))$. The inducing variables are used to sparsely represent the Gaussian process vector field \mathbf{f} , which reduces the complexity of the Gaussian process inference, i.e.,

$$\begin{aligned} p(\mathbf{f}|U) &= \mathcal{N}(K(\mathbf{x}(t), Z)K^{-1}(Z, Z')U, \\ &K(\mathbf{x}(t), \mathbf{x}(t')) - K(\mathbf{x}(t), Z)K^{-1}(Z, Z')K(Z, \mathbf{x}(t))) \end{aligned} \quad (11)$$

where $K(Z, Z')$ is the covariance matrix between the inducing points Z and Z' . Like most of the previous works [Titsias, 2009; Hensman *et al.*, 2015], here we assume that the joint approximate posterior distribution for the Gaussian process can be expressed as:

$$q(\mathbf{f}, U) = q(\mathbf{f}|U)q(U) = p(\mathbf{f}|U)q(U) \quad (12)$$

Let us consider the ODE model proposed in Eq. (10) augmented by sparse inducing points presented in Eq. (11). In Bayesian statistics, a vital object of learning and inference is the model evidence function $p(Y)$. For instance, Bayesian learning typically resorts to maximizing the logarithm of the model evidence function $p(Y)$. By imposing constraints on the model parameters θ during the maximization process, such as introducing regularization terms, the trade-off between data fit and model complexity can be balanced to obtain a more appropriate model.

$$\log p(Y) \geq \mathcal{L}(\theta) = \mathbb{E}_{q(\mathbf{x}(0), \mathbf{f}, U)} \left[\log \frac{p(\mathbf{f}, U, \mathbf{x}(0), Y)}{q(\mathbf{x}(0), \mathbf{f}, U)} \right] \quad (13)$$

where $\theta = \{q(U), q(\mathbf{x}(0)), G_K, \lambda\}$, $q(U), q(\mathbf{x}(0))$ are respectively variational posterior of U and $\mathbf{x}(0)$, λ is other model parameters such as Gaussian kernel lengthscale. We use the ELBO as the objective function to optimize the variational distribution $q(U)$. With the application of mathematical techniques such as Jensen's inequality, Eq. (13) can be

mathematically simplified to:

$$\begin{aligned} \mathcal{L}(\theta) &= \underbrace{\mathbb{E}_{q(\mathbf{f}), q(\mathbf{x}(0))} [\log p(Y|G_K \circ \mathbf{f}, \mathbf{x}(0))]}_{\text{the data reconstruction error}} \\ &- \underbrace{KL[q(U)||p(U)]}_{\text{the regularization term for } q(U)} - \underbrace{KL[q(\mathbf{x}(0))||p(\mathbf{x}(0))]}_{\text{the regularization term for } q(\mathbf{x}(0))} \end{aligned} \quad (14)$$

where $\mathbb{E}_{q(\mathbf{f}), q(\mathbf{x}(0))} [\log p(Y|G_K \circ \mathbf{f}, \mathbf{x}(0))]$ is the expected log-likelihood of the data under the variational distribution $q(\mathbf{f})$, and $q(\mathbf{x}(0))$. Specially, $q(\mathbf{f}) = \int q(\mathbf{f}, U) dU$ is sampled from the variational posterior using Matheron's Rule [Wilson *et al.*, 2020], as detailed in Appendix. In addition, we can write the likelihood function explicitly as:

$$p(Y|G_K \circ \mathbf{f}, \mathbf{x}(0)) = \mathcal{N}(\mathbf{x}(0) + \int_0^t G_K \circ \mathbf{f}(\mathbf{x}(\tau)) d\tau, R) \quad (15)$$

We optimize the ELBO using a stochastic gradient descent based method, where the gradients are computed using Monte Carlo sampling. The integral in Equation (15) can be solved using an ODE solver. Specifically, as mentioned in Section 3.1, in order to obtain a more accurate estimation of the model's uncertainty, we parameterize the variational distribution $q(U)$ in Eq. (14) with another normalizing flow. For example, if the Planar Flow is used, then,

$$\begin{aligned} U &= \phi(V) \\ q(U) &= \pi(V) \times \left| \det \left(\frac{d\phi}{dV} \right) \right|^{-1} = \pi(V) \times |1 + \mathbf{u}^\top \psi(V)|^{-1} \end{aligned} \quad (16)$$

where V is a new random variable with a standard normal distribution $\pi(\cdot) = \mathcal{N}(\mathbf{0}, I)$. Then using Eq. (16), the KL divergence in Eq. (14) can be re-written as:

$$\begin{aligned} &KL(q(U) || p(U)) \\ &= \mathbb{E}_{q(U)} [\log q(U) - \log p(U)] \\ &= \mathbb{E}_{\pi(V)} [\log \pi(V) - \log \left| \det \left(\frac{d\phi}{dV} \right) \right| - \log p(\phi(V))] \\ &= -\mathbb{E}_{\pi(V)} \log \left| \det \left(\frac{d\phi}{dV} \right) \right| - \mathbb{E}_{\pi(V)} \log p(\phi(V)) + const. \\ &= -\mathbb{E}_{\pi(V)} \log |1 + \mathbf{u}^\top \psi(V)| + \frac{1}{2} \log |K(Z, Z')| \\ &+ \frac{1}{2} \mathbb{E}_{\pi(V)} U^T K^{-1}(Z, Z') U + const \end{aligned} \quad (17)$$

We can still utilize Monte Carlo sampling to obtain an unbiased estimate of the KL term from the Eq. (17). Considering that inference of $q(\mathbf{x}(0))$ is relatively easy, we can use a simple Gaussian distribution, i.e., $q(\mathbf{x}(0)) = \mathcal{N}(\mu_0, \Sigma_0)$. By combining Eq. (14) and (17), we construct the complete objective function for double normalizing flows.

4 Experiments

In this section, we conduct a comprehensive evaluation of our approach against state-of-the-art methods including Bayesian

Method	Task 1: MNLL	Task 1: MSE	Task 2: MNLL	Task 2: MSE
Bayesian NeuralODE	0.82 ± 0.01	1.45 ± 0.04	0.88 ± 0.01	1.68 ± 0.04
NeuralODE	-	0.29 ± 0.11	-	0.55 ± 0.07
npODE	1.47 ± 0.59	0.16 ± 0.05	8.89 ± 3.06	2.08 ± 0.78
GPODE	0.60 ± 0.03	0.13 ± 0.01	0.41 ± 0.18	0.21 ± 0.07
ODE2VAE	0.55 ± 0.03	0.13 ± 0.01	0.37 ± 0.14	0.19 ± 0.05
Latent SDE	0.42 ± 0.03	0.10 ± 0.01	0.30 ± 0.18	0.15 ± 0.05
DNF (ours)	0.12 ± 0.01	0.031 ± 0.01	0.21 ± 0.06	0.04 ± 0.01

Table 1: Performance Metrics for Regular and Irregular Time-grids in the VDP Dynamic

NeuralODE [Dandekar *et al.*, 2020], NeuralODE [Chen *et al.*, 2018], npODE [Heinonen *et al.*, 2018], GPODE [Hegde *et al.*, 2022], ODE2VAE [Yildiz *et al.*, 2019] and Latent SDE [Solin *et al.*, 2021] in diverse scenarios that encompass various challenges, including time series prediction, handling missing observations, and learning complex long trajectories. Our empirical results demonstrate that our model surpasses existing methods in terms of accuracy, while adeptly capturing the uncertainty associated with autonomous dynamics.

Method	MNLL	MSE
Bayesian NeuralODE	0.77 ± 0.12	0.24 ± 0.03
NeuralODE	-	0.18 ± 0.00
npODE	6.49 ± 1.49	0.08 ± 0.01
GPODE	0.09 ± 0.05	0.07 ± 0.02
ODE2VAE	0.09 ± 0.04	0.07 ± 0.02
Latent SDE	0.07 ± 0.03	0.05 ± 0.02
DNF (ours)	0.05 ± 0.02	0.04 ± 0.01

Table 2: Performance Metrics for Missing Data Learning in the FHN Dynamical System

4.1 Experiment Details

We illustrate the performance of our model on three benchmark datasets: VAN DER POL (VDP) dynamics [Kanamaru, 2007], FitzHughNagumo (FHN) systems [Aqil *et al.*, 2012] and human motion dynamics CMU MoCap database¹. We use 16 inducing points in VDP and FHN experiments and 100 inducing points for the MoCap experiments. We assume Gaussian observation likelihood, and infer the observe noise parameter from the training data. All the experiments use squared exponential kernel along with 256 Fourier basis functions for weight-space GP sampling methods as describe in the Appendix. Along with the variational parameters, normalizing flows parameters, kernel lengthscales, signal variance, noise scale, and inducing locations are jointly optimized against the model ELBO while training. We quantify the model fit by computing the expected negative log-likelihood (NLL) of the data points under the predictive distribution and the mean squared error (MSE) between ground

truth. All the experiments are repeated with random initialization, and means and standard errors are reported over 10 runs. For all experiments, we employ the RK4 ODE solver [Schober *et al.*, 2014] and the torchdiffeq library [Chen *et al.*, 2018] for integration and gradient computation. We determine the other hyperparameters through grid search. Specifically, we use five layers of Planar flows for the prior and three layer of Planar flow for the posterior to jointly infer the posterior distribution of the inducing variables.

4.2 Time Series Prediction of Simulated Dynamical Systems.

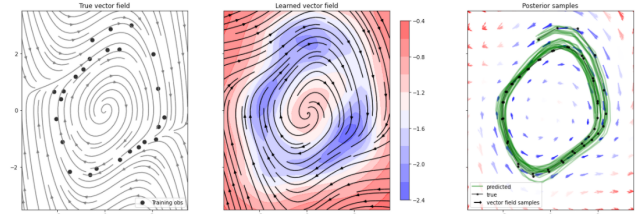


Figure 1: In order, they respectively represent: the true vector field, learned from the VDP dynamical system and the posterior trajectories of sampled particles by our DNF method. The log variance gradually decreases from red to blue.

We initially demonstrate the effectiveness of our proposed method by incorporating double normalizing flows (DNFs) into the vector field of a two-dimensional Van der Pol (VDP) system.

$$\begin{aligned} \dot{x}_1 &= x_2, \\ \dot{x}_2 &= -x_1 + 0.5x_2(1 - x_1^2). \end{aligned} \quad (18)$$

We generated a trajectory of 50 states by simulating the true system dynamics from the initial state $(x_1(0), x_2(0)) = (-1.5, 2.5)$, and added Gaussian noise with $\sigma^2 = 0.05$ to generate the training data. We then explored two scenarios with different training time intervals, $t \in [0, 7]$ and forecasting intervals $t \in [7, 14]$ respectively, using a regularly sampled time grid (Task 1) and an irregular grid (Task 2) with uniform random sampling of time points.

From Table 1, it can be observed that our proposed method exhibits lower MSE and MNLL values compared to the other five methods. Moreover, Fig. 1 shows the vector field learned from the proposed method and sampled trajectories from the

¹<http://mocap.cs.cmu.edu/>

Method	Subject 09short	Subject 09long	Subject 35short	Subject 35long	Subject 39short	Subject 39long
Bayesian NeuralODE	2.03 ± 0.10	1.50 ± 0.05	1.42 ± 0.05	1.37 ± 0.06	1.61 ± 0.07	1.45 ± 0.03
npODE	2.09 ± 0.01	1.78 ± 0.08	1.67 ± 0.02	1.66 ± 0.04	2.06 ± 0.05	1.78 ± 0.04
GPODE	1.19 ± 0.02	1.14 ± 0.02	1.25 ± 0.06	1.08 ± 0.04	1.25 ± 0.01	1.36 ± 0.02
ODE2VAE	1.17 ± 0.02	1.12 ± 0.02	1.21 ± 0.05	1.05 ± 0.04	1.23 ± 0.01	1.31 ± 0.02
Latent SDE	1.05 ± 0.02	1.00 ± 0.02	0.95 ± 0.05	0.86 ± 0.04	1.08 ± 0.01	1.18 ± 0.02
DNF (ours)	0.98 ± 0.02	0.96 ± 0.02	0.82 ± 0.04	0.79 ± 0.03	1.02 ± 0.01	1.10 ± 0.02

Table 3: MNLL for Long Sequences and Short Sequences Learning

Method	Subject 09short	Subject 09long	Subject 35short	Subject 35long	Subject 39short	Subject 39long
Bayesian NeuralODE	25.50 ± 1.70	21.32 ± 2.58	23.09 ± 3.95	20.86 ± 2.95	53.34 ± 5.31	39.66 ± 6.82
npODE	27.53 ± 2.87	33.83 ± 2.46	36.50 ± 3.86	23.54 ± 0.56	115.38 ± 10.96	53.51 ± 2.98
GPODE	9.11 ± 0.37	8.38 ± 1.23	10.11 ± 0.79	11.66 ± 0.73	26.72 ± 0.63	21.17 ± 2.88
ODE2VAE	9.05 ± 0.32	8.14 ± 1.05	9.25 ± 0.96	10.08 ± 1.07	25.25 ± 0.61	21.06 ± 2.14
Latent SDE	7.46 ± 0.30	6.45 ± 0.54	7.57 ± 0.46	7.65 ± 0.55	21.25 ± 0.32	18.72 ± 0.97
DNF(ours)	7.03 ± 0.24	6.04 ± 0.45	6.72 ± 0.22	7.03 ± 0.23	19.43 ± 0.26	16.21 ± 0.73

Table 4: MSE for Long Sequences and Short Sequences Learning

posterior of this vector field. The experimental results emphasize the effectiveness and superiority of DNF in synthesizing data sets for time series prediction.

4.3 Missing Observations Learning of Simulated Dynamical Systems

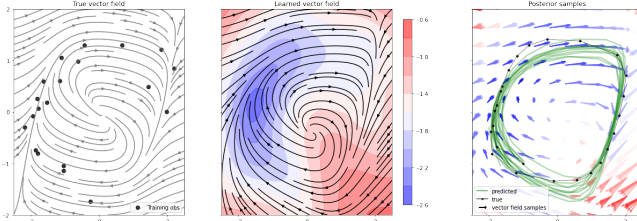


Figure 2: In order, they respectively represent: the true vector field, the vector field learned from the FHN dynamical system and the posterior trajectories of sampled particles. The log variance gradually decreases from red to blue.

We continue to evaluate the impact of double normalizing flows on our model’s on the performance of our model in time series recovery task using the FitzHugh-Nagumo FHN oscillator,

$$\begin{aligned} \dot{x}_1 &= 3(x_1 - x_1^3/3 + x_2), \\ \dot{x}_2 &= (0.2 - 3x_1 - 0.2x_2)/3. \end{aligned} \quad (19)$$

We first generate a training sequence with 25 regularly-sampled time points from $t \in [0, 5.0]$ and adding Gaussian noise with $\sigma^2 = 0.025$. Afterwards, we remove all observations in the quadrant where $x_1 > 0$ and $x_2 < 0$, and assess the accuracy of our model in this region. Fig. 2 showcases the learned vector field and sampled trajectories from the posterior of this vector field. Based on the results in Table 2, our model has demonstrated significant improvements in performance compared to the previous methods on the missing data task.

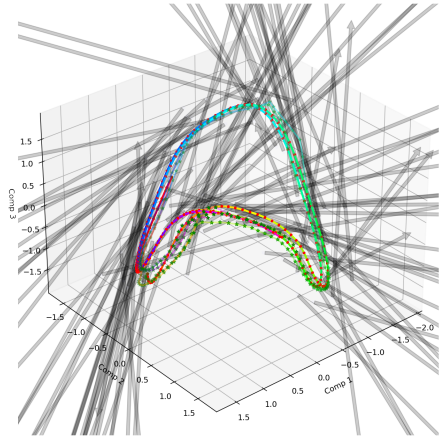


Figure 3: A 3D model for learned vector field in the PCA latent space.

4.4 Complex Trajectories Learning for Real-world Datasets

Next, to evaluate the effectiveness of double normalizing flows, we apply our approach to learn the dynamics of human motion from noisy experimental data obtained from the CMU MoCap database for three subjects (09, 35, and 39). The dataset consists of 50 sensor readings from different body parts while subjects are walking or running. Following the preprocessing approach of most previous methods, we center the data and further split it into train, test, and validation sequences. To reduce the dimensionality of the data, we project the original 50-dimensional data into a 5-dimensional latent space using Principal Component Analysis (PCA) and learn the dynamics in the latent space. We conduct separate tests of our model’s effectiveness on long sequences and short sequences. Additionally, we use multiple shooting method as describe in the Appendix and considered the number of shooting segments to be the same as the number of observation segments in the dataset.

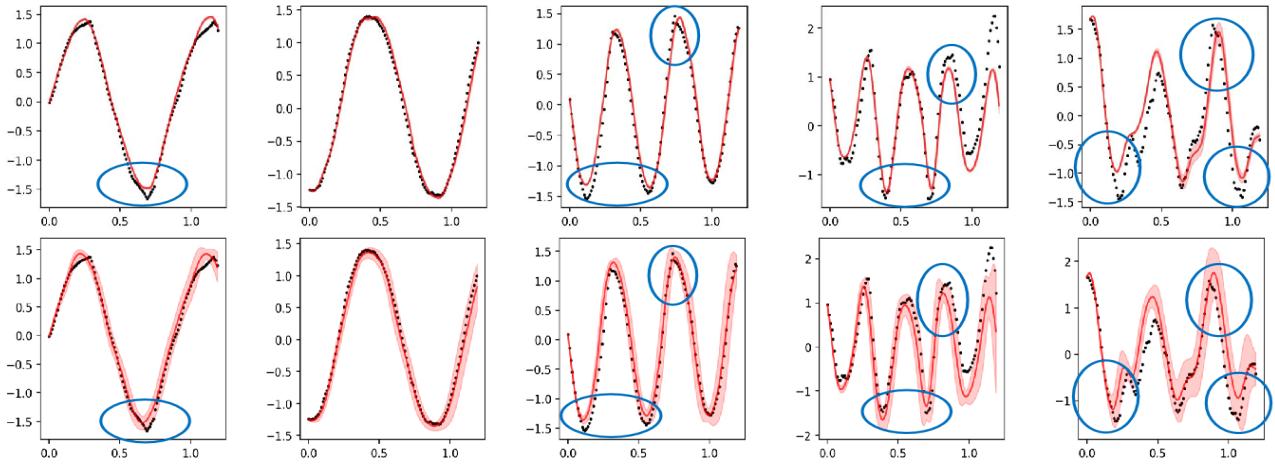


Figure 4: we compared the results of the GPODE method and our DNF method. The top row shows the results of GPODE, while the bottom row shows the results of our DNF method. The black dashed line represents the true testing dataset, with time on the x-axis and data values on the y-axis. The deep red solid line represents the predicted mean value, and the light red shaded area represents the 95% credible interval used to assess uncertainty. We have also highlighted two areas of difference between the two methods with deep blue circles. Additionally, our method has a coverage probability of 0.60, while GPODE has a coverage probability of 0.81.

We first project the data into a 5-dimensional latent space using PCA, and then we apply the double normalizing flows approach in the latent space. In Fig. 3, we showcase the sampling of inducing points and particle trajectories in the latent space using a 3D model. To compute the data likelihood, we project the latent dynamics back to the original data space by inverting the PCA. We evaluate the predictive performance on unseen test sequences of our approach against other state-of-the-art methods on MLL and MSE metrics in Tables 3 and 4, respectively. The results demonstrate that our approach achieves higher experimental accuracy and better uncertainty estimation on complex datasets.

In addition, to demonstrate the necessity of using double normalization flow, we will also report the coverage probability. The coverage probability measures the proportion of true values within the 95% confidence interval, thereby evaluating the uncertainty estimation in our time series prediction task on the MoCap09 test set. By visualizing the coverage probability in Figure 4, we showcase our prediction results that our DNF method outperforms previous GPODEs. Specially, we can also observe that, compared to previous GPODE methods, our method captures the details of complex data more accurately. To highlight the visual differences between the two approaches, we mark them with blue circles. This improvement, along with the comparison of NMLL in Tables 3, indicates that DNFs are capable of providing better uncertainty estimation and generalization capability from another perspective.

4.5 Time Analysis

Although our DNF method has improved the performance compared to the previous GPODE method, the introduction of new parameters for learning and inference has led to additional time complexity. Therefore, we have included a new table that provides a comparison between our proposed model and the baseline model on the Mocap dataset. This table

provides a comprehensive comparison of the time consumption between the two algorithms after 500 iterations on the NVIDIA A100 platform. It can be observed that as the dataset size increases, the primary computational resources are allocated towards handling other components, rather than computing the normalizing flows. As a result, our model demonstrates higher adaptability to changes in dataset size, and is not significantly affected by its increase.

Dataset	Mocap09	Mocap35	Mocap39
GPODE	210.5s	435.3s	187.2s
DNF (ours)	169.7s	412.1s	158.7s

Table 5: Comparison of the time consumption between GPODE and DNF after 500 iterations

5 Conclusion

This paper elaborates on the improvements of double normalizing flow (DNF) for the GP-ODE model in terms of accuracy and uncertainty estimation from both theoretical and experimental perspectives. The method leverages the flexibility and analyticity of normalizing flows, emphasizing their roles in characterizing probability vector fields and particle trajectory behaviors. However, there are limitations to this method, such as the selection of hyperparameters and the need to carefully apply techniques such as early stopping and regularization to prevent potential overfitting issues, as well as numerical stability concerns related to the KL regularization term. Addressing these challenges remains a task, nevertheless, double normalizing flow undoubtedly presents a promising and flexible approach with significant potential in both theory and practical applications, worthy of adoption in the field.

References

- [Aqil *et al.*, 2012] Muhammad Aqil, Keum-Shik Hong, and Myung-Yung Jeong. Synchronization of coupled chaotic fitzhugh–nagumo systems. *Communications in Nonlinear Science and Numerical Simulation*, 17(4):1615–1627, 2012.
- [Bishop and Nasrabadi, 2006] Christopher M Bishop and Nasser M Nasrabadi. *Pattern recognition and machine learning*, volume 4. Springer, 2006.
- [Blei *et al.*, 2017] David M Blei, Alp Kucukelbir, and Jon D McAuliffe. Variational inference: A review for statisticians. *Journal of the American statistical Association*, 112(518):859–877, 2017.
- [Chen *et al.*, 2018] Ricky TQ Chen, Yulia Rubanova, Jesse Bettencourt, and David K Duvenaud. Neural ordinary differential equations. *Advances in neural information processing systems*, 31, 2018.
- [Chen *et al.*, 2022] Xing Chen, Flavio Abreu Araujo, Mathieu Riou, Jacob Torrejon, Dafiné Ravelosona, Wang Kang, Weisheng Zhao, Julie Grollier, and Damien Querlioz. Forecasting the outcome of spintronic experiments with neural ordinary differential equations. *Nature communications*, 13(1):1016, 2022.
- [Dandekar *et al.*, 2020] Raj Dandekar, Karen Chung, Vaibhav Dixit, Mohamed Tarek, Aslan Garcia-Valadez, Krishna Vishal Vemula, and Chris Rackauckas. Bayesian neural ordinary differential equations. *arXiv preprint arXiv:2012.07244*, 2020.
- [Deng *et al.*, 2020] Ruizhi Deng, Bo Chang, Marcus A Brubaker, Greg Mori, and Andreas Lehrmann. Modeling continuous stochastic processes with dynamic normalizing flows. *Advances in Neural Information Processing Systems*, 33:7805–7815, 2020.
- [Deng *et al.*, 2021] Ruizhi Deng, Marcus A Brubaker, Greg Mori, and Andreas Lehrmann. Continuous latent process flows. *Advances in Neural Information Processing Systems*, 34:5162–5173, 2021.
- [Du *et al.*, 2022] Shian Du, Yihong Luo, Wei Chen, Jian Xu, and Delu Zeng. To-flow: Efficient continuous normalizing flows with temporal optimization adjoint with moving speed. In *Proceedings of the IEEE/CVF Conference on Computer Vision and Pattern Recognition*, pages 12570–12580, 2022.
- [Fortuin, 2022] Vincent Fortuin. Priors in bayesian deep learning: A review. *International Statistical Review*, 90(3):563–591, 2022.
- [Hegde *et al.*, 2018] Pashupati Hegde, Markus Heinonen, Harri Lähdesmäki, and Samuel Kaski. Deep learning with differential gaussian process flows. *arXiv preprint arXiv:1810.04066*, 2018.
- [Hegde *et al.*, 2022] Pashupati Hegde, Çağatay Yıldız, Harri Lähdesmäki, Samuel Kaski, and Markus Heinonen. Variational multiple shooting for bayesian odes with gaussian processes. In *Uncertainty in Artificial Intelligence*, pages 790–799. PMLR, 2022.
- [Heinonen *et al.*, 2018] Markus Heinonen, Çağatay Yıldız, Henrik Mannerström, Jukka Intosalmi, and Harri Lähdesmäki. Learning unknown ode models with gaussian processes. In *International Conference on Machine Learning*, pages 1959–1968. PMLR, 2018.
- [Hensman *et al.*, 2015] James Hensman, Alexander Matthews, and Zoubin Ghahramani. Scalable variational gaussian process classification. In *Artificial Intelligence and Statistics*, pages 351–360. PMLR, 2015.
- [Hu *et al.*, 2021] Caie Hu, Sanyou Zeng, Changhe Li, and Fei Zhao. On nonstationary gaussian process model for solving data-driven optimization problems. *IEEE Transactions on Cybernetics*, 2021.
- [Kanamaru, 2007] Takashi Kanamaru. Van der pol oscillator. *Scholarpedia*, 2(1):2202, 2007.
- [Kobyzev *et al.*, 2020] Ivan Kobyzev, Simon JD Prince, and Marcus A Brubaker. Normalizing flows: An introduction and review of current methods. *IEEE transactions on pattern analysis and machine intelligence*, 43(11):3964–3979, 2020.
- [Liu *et al.*, 2020] Haitao Liu, Yew-Soon Ong, Xiaobo Shen, and Jianfei Cai. When gaussian process meets big data: A review of scalable gps. *IEEE transactions on neural networks and learning systems*, 31(11):4405–4423, 2020.
- [Lüders *et al.*, 2022] Christoph Lüders, Thomas Sturm, and Ovidiu Radulescu. Odebase: a repository of ode systems for systems biology. *Bioinformatics Advances*, 2(1):vbac027, 2022.
- [Mao and Sun, 2020] Liang Mao and Shiliang Sun. Multiview variational sparse gaussian processes. *IEEE Transactions on Neural Networks and Learning Systems*, 32(7):2875–2885, 2020.
- [Maroñas *et al.*, 2021] Juan Maroñas, Oliver Hamelijnck, Jeremias Knoblauch, and Theodoros Damoulas. Transforming gaussian processes with normalizing flows. In *International Conference on Artificial Intelligence and Statistics*, pages 1081–1089. PMLR, 2021.
- [Oksendal, 2013] Bernt Oksendal. *Stochastic differential equations: an introduction with applications*. Springer Science & Business Media, 2013.
- [Papamakarios *et al.*, 2021] George Papamakarios, Eric Nalisnick, Danilo Jimenez Rezende, Shakir Mohamed, and Balaji Lakshminarayanan. Normalizing flows for probabilistic modeling and inference. *The Journal of Machine Learning Research*, 22(1):2617–2680, 2021.
- [Rasul *et al.*, 2020] Kashif Rasul, Abdul-Saboor Sheikh, Ingmar Schuster, Urs Bergmann, and Roland Vollgraf. Multivariate probabilistic time series forecasting via conditioned normalizing flows. *arXiv preprint arXiv:2002.06103*, 2020.
- [Rezende and Mohamed, 2015] Danilo Rezende and Shakir Mohamed. Variational inference with normalizing flows. In *International conference on machine learning*, pages 1530–1538. PMLR, 2015.

- [Schober *et al.*, 2014] Michael Schober, David K Duvenaud, and Philipp Hennig. Probabilistic ode solvers with runge-kutta means. *Advances in neural information processing systems*, 27, 2014.
- [Solin *et al.*, 2021] Arno Solin, Ella Tamir, and Prakhar Verma. Scalable inference in sdes by direct matching of the fokker–planck–kolmogorov equation. *Advances in Neural Information Processing Systems*, 34:417–429, 2021.
- [Sommerfeld, 1949] Arnold Sommerfeld. *Partial differential equations in physics*. Academic press, 1949.
- [Tenenbaum and Pollard, 1985] Morris Tenenbaum and Harry Pollard. *Ordinary differential equations: an elementary textbook for students of mathematics, engineering, and the sciences*. Courier Corporation, 1985.
- [Titsias, 2009] Michalis Titsias. Variational learning of inducing variables in sparse gaussian processes. In *Artificial intelligence and statistics*, pages 567–574. PMLR, 2009.
- [Wilson *et al.*, 2020] James Wilson, Viacheslav Borovitskiy, Alexander Terenin, Peter Mostowsky, and Marc Deisenroth. Efficiently sampling functions from gaussian process posteriors. In *International Conference on Machine Learning*, pages 10292–10302. PMLR, 2020.
- [Yang *et al.*, 2019] Guandao Yang, Xun Huang, Zekun Hao, Ming-Yu Liu, Serge Belongie, and Bharath Hariharan. Pointflow: 3d point cloud generation with continuous normalizing flows. In *Proceedings of the IEEE/CVF international conference on computer vision*, pages 4541–4550, 2019.
- [Yildiz *et al.*, 2019] Cagatay Yildiz, Markus Heinonen, and Harri Lahdesmaki. Ode2vae: Deep generative second order odes with bayesian neural networks. *Advances in Neural Information Processing Systems*, 32, 2019.
- [Zhang and Chen, 2021] Qinsheng Zhang and Yongxin Chen. Diffusion normalizing flow. *Advances in Neural Information Processing Systems*, 34:16280–16291, 2021.
- [Zhang *et al.*, 2018] Cheng Zhang, Judith Bütetpage, Hedvig Kjellström, and Stephan Mandt. Advances in variational inference. *IEEE transactions on pattern analysis and machine intelligence*, 41(8):2008–2026, 2018.
- [Zhang *et al.*, 2022] Baoquan Zhang, Xutao Li, Shanshan Feng, Yunming Ye, and Rui Ye. Metanode: Prototype optimization as a neural ode for few-shot learning. In *Proceedings of the AAAI Conference on Artificial Intelligence*, volume 36, pages 9014–9021, 2022.
- [Zhi *et al.*, 2022] Weiming Zhi, Tin Lai, Lionel Ott, Edwin V Bonilla, and Fabio Ramos. Learning efficient and robust ordinary differential equations via invertible neural networks. In *International Conference on Machine Learning*, pages 27060–27074. PMLR, 2022.
- [Zhu *et al.*, 2022] Aiqing Zhu, Pengzhan Jin, Beibei Zhu, and Yifa Tang. On numerical integration in neural ordinary differential equations. In *International Conference on Machine Learning*, pages 27527–27547. PMLR, 2022.